New Skyrme interaction for normal and exotic nuclei

B. Alex Brown
Department of Physics and Astronomy and National Superconducting Cyclotron Laboratory, Michigan State University, East Lansing, Michigan 48824-1321
and Department of Physics, University of Stellenbosch, Stellenbosch 7600, South Africa
(Received 5 May 1997)

A new set of Skyrme parameters is obtained from a fit to the binding energies, rms charge radii, and single-particle energies of both normal and exotic spherical nuclei. Nuclear matter and neutron matter properties are used to put constraints on the parameters which are not well determined from the nuclear data. Special problems with the Nolen-Schiffer anomaly and the spin-orbit interaction are discussed. [S0556-2813(98)02107-4]

PACS number(s): 21.10.Dr, 21.10.Pc, 21.30.Fe, 21.60.Cs

I. INTRODUCTION

Since the implementation of the Skyrme interaction [1] by Vautherin and Brink [2], this model has proven remarkably useful and successful for nuclear Hartree-Fock (HF) calculations. It appears to incorporate the essential physics in terms of a minimal set of parameters, e.g., an s- and p-wave expansion of an effective nucleon-nucleon interaction together with a density-dependent part which accounts for the truncation of the shell-model space to a closed-shell configuration as well as for three-body interactions. Since the interaction is phenomenological, the parameters need to be determined from experimental data.

In the present paper I discuss a fit of the Skyrme parameters to a large body of data related to nuclear ground state properties. These include binding energies, rms charge radii, and single-particle energies. It is important to achieve good agreement for the single-particle energies of the most exotic nuclei measured in order to improve the reliability for predictions of the properties of even more exotic nuclei out to the proton and neutron drip lines. I consider these properties for the spherical nuclei ^{16}O, ^{24}O, ^{34}Si, ^{40}Ca, ^{48}Ca, ^{48}Ni, ^{68}Ni, ^{88}Sr, ^{100}Sn, ^{132}Sn, and ^{208}Pb. This set includes the most exotic nuclei studied to date. Although ^{16}O and ^{40}Ca are included in this list (as they have been since the first determinations of the Skyrme parameters), I will show that their single-particle spectra are not as well described as the other nuclei considered.

The data considered are well reproduced by varying six out of the ten conventional Skyrme-interaction parameters. Constraints on the four poorly determined parameters are obtained by comparison to nuclear matter and neutron matter properties. In addition, I modify the usual Skyrme interaction to allow for a more general spin-orbit potential and to take into account the Nolen-Schiffer displacement energy anomaly. The single-particle energy data give some preference for using the isoscalar (relativistic) form for the spin-orbit potential. The Nolen-Schiffer anomaly can be taken into account by introducing an isovector effective mass or by removing the Coulomb exchange term.

The main new ingredient in this work which distinguishes it from the many other works on the Skyrme interaction which exist in the literature is the emphasis on the single-particle energies. Previous investigations have been concerned with general aspects of the single-particle energies such as the spin-orbit splitting and the level density at the Fermi surface, but they have not treated the fits to these data in a quantitative way. The second ingredient is a consistent formulation for both proton-rich and neutron-rich nuclei which requires an understanding of the Nolen-Schiffer anomaly. The last two ingredients follow suggestions which have been discussed previously (specific references will be given below); a generalized form for spin-orbit interaction and constraints on the Skyrme parameters which are related to nuclear matter and neutron matter properties.

The form for the Skyrme interaction is summarized in Sec. II, and the experimental data used for the fit are discussed in Sec. III. Section IV deals with the special problem for the mirror displacement energies, since the physics involved can be largely separated from the other aspects. The general fit results are discussed in Sec. V including the details about the spin-orbit interaction and the constraints to nuclear matter and neutron matter. Results for the binding energies and single-particle energies are discussed in Sec. VI, and results for the rms charge radii and densities are discussed in Sec. VII. The conclusions are given in Sec. VIII.

II. FORM OF THE SKYRME INTERACTION

For the central potential I use the standard form of Vautherin and Brink [2] with the addition of the x_1, x_2, and x_3 exchange terms and the ρ^α density dependence [3–9]:

$$V_{\rm Skyrme}=t_0(1+x_0P_\sigma)\,\delta+\frac{1}{2}t_1(1+x_1P_\sigma)(\mathbf{k}'^2\delta+\delta\mathbf{k}^2)$$
$$+t_2(1+x_2P_\sigma)\mathbf{k}'\cdot\delta\mathbf{k}+\frac{1}{6}t_3(1+x_3P_\sigma)\rho^\alpha(\mathbf{R})\,\delta, \tag{1}$$

where $\delta=\delta(\mathbf{r}_i-\mathbf{r}_j)$, $\mathbf{k}=(1/2i)(\nabla_i-\nabla_j)$ is the relative momentum operator acting on the wave function to the right and $\mathbf{k}'$ is the adjoint of $\mathbf{k}$. P_σ is the spin-exchange operator and $\mathbf{R}=(\mathbf{r}_i+\mathbf{r}_j)/2$.

The spin-orbit potential is the one obtained from the two-body interaction of Vautherin and Brink as modified by Sharma *et al.* [10]:

$$V_{\rm so}=iW_0(1+x_wP_\tau)\mathbf{k}'\cdot\delta(\boldsymbol{\sigma}\times\mathbf{k}). \tag{2}$$

P_τ is the isospin-exchange operator and $\sigma=\sigma_1+\sigma_2$ where σ_i are the Pauli spin matricies. As in Ref. [10] the one-body spin-orbit potential is constructed without the exchange (Fock) term. Equation (2) with $x_w=1$ is the original two-body interaction of Vautherin and Brink which gives a one-body spin-orbit potential proportional to $2J_p+J_n$ for protons and proportional to J_p+2J_n for neutrons, where J_p and J_n are the proton and neutron spin densities. Equation (2) with $x_w=0$ gives a one-body spin-orbit potential for both protons and neutrons which is proportional to the scalar spin density J_p+J_n. This scalar form is close to that obtained in the relativistic mean-field model [10], and also to the form usually assumed for the one-body Woods-Saxon potential.

The direct part of the Coulomb interaction is obtained from the charge distribution $\rho_{\rm ch}$. For the exchange part of the Coulomb interaction I use the approximation [8]

$$V_{\rm Coul,exch}=-x_ce^2\left(\frac{3}{\pi}\right)^{1/3}\rho_{\rm ch}^{1/3}, \tag{3}$$

where x_c is a parameter which can be used to turn off the exchange part ($x_c=0$). The charge distributions are obtained by folding the point nucleon distributions with the proton and neutron charge distributions and includes the center-of-mass and the spin-orbit corrections [9,11]. The Coulomb potential is calculated from a point proton distribution whose density distribution is adjusted to match the calculated charge rms radius. The single-particle energies obtained from this approximation differ from the exact ones obtained from the full charge distribution by about 20 keV or less and the total binding energy for ^{208}Pb differs by 400 keV from the exact one. In terms of the fit, these differences are absorbed into the parameters. In the final iteration the exact charge distribution is calculated for the comparison to experiment.

The free-nucleon masses are used for the single-particle HF kinetic energies, and the center-of-mass correction to the kinetic energy is evaluated by subtracting the expectation value of the center-of-mass kinetic energy in the harmonic oscillator approximation

$$E_{\rm c.m.}=\left\langle\frac{P^2}{2Am}\right\rangle=\frac{3}{4}\hbar\omega, \tag{4}$$

with $\hbar\omega=45A^{-1/3}-25A^{-2/3}$.

III. DATA FOR DOUBLY CLOSED SHELL NUCLEI

The Skyrme parameters are obtained by minimizing the χ value given by

$$\chi^2=\sum_i w_i^2(d_i^{\rm exp}-d_i^{\rm th})^2/[(N_d-N_p)], \tag{5}$$

where the sum runs over the i data points d_i, $w_i=1/\sigma_i$ is the theoretical weight corresponding to the theoretical ''error'' σ_i, N_d is the number of data, and N_p is the number of parameters.

The eleven nuclei considered in this work are ^{16}O, ^{24}O, ^{34}Si, ^{40}Ca, ^{48}Ca, ^{48}Ni, ^{68}Ni, ^{88}Sr, ^{100}Sn, ^{132}Sn, and ^{208}Pb. All of these except ^{48}Ni and ^{100}Sn have measured binding energies with an error of 300 keV or less [12]. The binding energy of ^{48}Ni can be extrapolated to within an error of about 200 keV based upon displacement energy systematics [13–15]. This data is treated in terms of the mirror binding energy difference BE(^{48}Ca) − BE(^{48}Ni) = 67.06 MeV. The binding energy of ^{100}Sn has recently been measured [16], BE = 825.8(9) MeV, and has a relatively large error.

These eleven nuclei are all characterized by having first excited levels which are significantly higher in energy compared to those of the neighboring even-even nuclei. They consist of those nuclei which are conventionally thought of as having good closed-shell configurations, corresponding to the major shell gaps at 8, 20, 50, and 82, for both protons and neutrons, ^{16}O, ^{40}Ca, ^{100}Sn, ^{132}Sn, and ^{208}Pb, plus those for which one type of nucleon has a large shell gap and the other type of nucleon has a minor (semimagic) shell gap (14, 28, and 38), ^{24}O, ^{34}Si, ^{48}Ca, ^{48}Ni, and ^{88}Sr. (The semimagic properties of ^{90}Zr and ^{88}Sr are rather similar, and only one of them is needed for the fit.) In addition, I include ^{68}Ni, even though both protons and neutrons are semimagic, in order to give some information in the fit from this region of nuclei.

All of the binding energies were assigned theoretical errors of $\sigma=1.0$ MeV for the fit, except for those of ^{132}Sn and ^{208}Pb which were given $\sigma=0.5$ MeV and for ^{100}Sn which was given its experimental error of $\sigma=0.9$ MeV. The smallest errors are assigned to ^{132}Sn and ^{208}Pb which are the best examples of doubly closed shell nuclei. For the nuclei ^{24}O, ^{34}Si and ^{48}Ca (^{48}Ni) it is possible to carry out 0 $\hbar\omega$ shell-model calculations [17,18] in order to investigate the ''local'' configuration mixing effect on the binding energies. These calculations give a correlation energy for these three nuclei (due to $T=1$ BCS-type correlations) of about 1.0 MeV. One might expect a similar correlation energy for the semimagic nuclei ^{68}Ni and ^{88}Sr. This is the main motivation of assigning 1.0 MeV theoretical errors to all of the nuclei. Even though ^{16}O and ^{40}Ca are usually thought of as good examples of doubly closed-shell nuclei, there is evidence that the correlations for these nuclei go beyond that which is implicit in the Skyrme Hartree-Fock potential. This will be discussed further in Sec. VI.

Even though I assume closed-shell Slater determinants for these nuclei, the correlations beyond the closed shell (such as two-particle two-hole admixtures) are always important, and one assumes that these correlations can be implicitly taken into account in terms of the effective parameters of the Skyrme interaction. The calculation of other observables such as electromagnetic transition rates must be explicitly renormalized to take into account the correlations.

In addition, the fit includes the rms charge radii [19] for ^{16}O (rms=2.737 fm, $\sigma=0.03$ fm), ^{40}Ca (rms=3.477 fm, $\sigma=0.03$ fm), ^{48}Ca (rms=3.474 fm, $\sigma=0.01$ fm), ^{88}Sr (rms =4.219 fm, $\sigma=0.01$ fm), and ^{208}Pb (rms=5.501 fm, σ =0.01 fm). Less weight is put on ^{16}O and ^{40}Ca, for the reasons discussed in Sec. VI.

I also include single-particle energies (SPE) in the fit. These include 14 levels for ^{16}O, ^{34}Si, and ^{40}Ca with $\sigma = 2.0$ MeV, 14 levels for ^{48}Ca and ^{88}Sr with $\sigma = 1.0$ MeV, four levels for ^{100}Sn with $\sigma = 1.0$ MeV which have been extrapolated from the properties of neighboring nuclei [20], 15 levels for ^{132}Sn with $\sigma = 0.5$ MeV and 22 levels for ^{208}Pb with $\sigma = 0.5$ MeV. Five of the loosely bound low-l SPE in ^{208}Pb and two of the loosely bound low-l SPE in ^{132}Sn where given a larger error of $\sigma = 1.0$ MeV for the reasons to be discussed in Sec. VI. The recently measured [21] levels in ^{133}Sn do not have measured spins, but I have adopted the suggested theoretical assignments from Ref. [21] which are consistent with the present calculations. The decreasing theoretical error as a function of mass reflects the larger spacing of energy levels in light nuclei compared to those in heavy nuclei, as well as the larger deviation between experiment and theory obtained for light nuclei (see Sec. VI).

The experimental value of the SPE is given by SPE $= E(A_0+1) - E^*(A_0)$, for particle (unfilled) states and SPE $= E(A_0) - E^*(A_0-1)$ for hole (filled) states, where $E(A_0)$ is the interaction energy of the even-even core, and E^* are the interaction energies for the ground or excited states of the neighboring odd-even nuclei. $E(A) = -\mathrm{BE}(A)$, where BE(A) is the binding energy which is defined to be a positive quantity. Most of these SPE are obtained from specific levels in the odd-even nuclei which have single-nucleon transfer spectroscopic factors which are large and close to the single-nucleon limit. In the cases of the very neutron-rich nuclei ^{34}Si and ^{132}Sn, the spectroscopic factors have not been measured, and I assume that the lowest-lying levels of a given spin and parity correspond to the expected ''single-particle'' states.

It is possible that any given single-particle state may be fragmented over several levels due to coupling with low-lying excited states of the core nuclei. However, these effects should be within the assigned theoretical error for the single-particle states considered for the fit. The exceptions to this are for the neutron deep-hole states in ^{207}Pb whose centroid energies are taken from Gales *et al.* [22] and the $0j_{15/2}$ neutron particle state in ^{209}Pb whose centroid energy was taken from the Table on page 573 of Nuclear Data Sheets compilation of Martin [23].

For the nuclei ^{24}O, ^{34}Si, and ^{48}Ca it is possible to carry out $0\hbar\omega$ shell-model calculations [17,18] in order to investigate the ''local'' configuration mixing effect on the single-particle energies. For all of these cases, the configuration mixing alters the single-particle energies by typically 500 keV or less. The largest change was found for the $0s_{1/2}$ hole state in ^{34}Si whose main component is in a state at 0.8 MeV in ^{33}Si but it partly fragmented over a state at 5.0 MeV (as yet unobserved since no transfer reactions have carried out for this unstable nucleus) moving its centroid energy lower in energy by about 0.8 MeV. In all cases the shifts expected from the shell-model configuration mixing are smaller than the errors assigned. The special nature of the fragmentation effects for ^{16}O and ^{40}Ca will be discussed further in Sec. VI.

If both kinds of nucleons are semimagic and $N=Z$, the $0\hbar\omega$ shell-model calculations give a large amount of mixing due to the strong proton-neutron interaction, and the closed-shell component of these nuclei is particularly small. Nuclei in this class which include ^{12}C [24], ^{28}Si [17], and ^{56}Ni [25] are not considered for the fit.

IV. THE DISPLACEMENT ENERGY ANOMALY FOR MIRROR NUCLEI

With the data set discussed in Sec. III, the largest contribution to the χ value is the ^{48}Ca-^{48}Ni binding energy difference which is theoretically too small compared to experiment by 3 to 5 MeV. This problem is related to the Nolen-Schiffer anomaly [26] which is usually discussed in terms of the displacement energies of mirror nuclei with with one valence nucleon ($T=1/2$), but it is magnified in this case by the large difference in proton number (eight) between ^{48}Ni and ^{48}Ca. Unless this difference is taken into account, there will be a problem with HF calculations for all nuclei across the $N=Z$ line.

For the typical HF calculation for ^{48}Ni, the $0f_{7/2}$ proton orbital is unbound by a few hundred keV. The calculation was carried out by artificially increasing the HF potential for the $0f_{7/2}$ orbit until it is bound by 0.2 MeV, and then using this wave function to calculate the expectation value of the Skyrme potential. Due to the large Coulomb barrier, the difference between the bound and quasibound wave functions is not large and I estimate an error of about 20 keV due to the approximation used. It is interesting to note that ^{48}Ni is one of best candidates for observing direct two-proton decay [13–15].

The Nolen-Schiffer anomaly is the observation that the magnitude of the experimental displacement energies of mirror nuclei are systematically 5 to 10% larger than those calculated. These calculations conventionally include the direct Coulomb interaction, the exchange Coulomb interaction, and the first-order core-polarization correction. The core-polarization correction, sometimes referred to as the Auerbach-Kahana-Weneser [27] (AKW) effect, is related to the small isovector potential in the core created by the Coulomb repulsion of the core protons. The AKW effect is automatically taken into account in the HF method when the valence orbitals are contained in the potential [28].

One way to account for the Nolen-Schiffer anomaly is to introduce a charge-asymmetric term in the nucleon-nucleon interaction. That is, the strong interaction is a little more attractive between two neutrons than it is between two protons. Experimental data on the charge-asymmetric interaction from nucleon-nucleon scattering has a large error due to the lack of precision in the neutron-neutron scattering experiments. I find that one can modify the proton-proton strength of the Skyrme interaction relative to the neutron-neutron strength to obtain better agreement for the ^{48}Ni-^{48}Ca binding energy difference. However, such modifications increase the contribution to the χ value from the other data in such a way that the total χ value does not change.

Another possible way to take into account the Nolen-Schiffer anomaly is to introduce a many-body (nuclear medium) correction to the Hamiltonian. One possibility that I have explored [29] is to make a small change in the isovector mass which appears in the kinetic energy operator, e.g., $\overline{m_p} = m_p(1+\delta_1)$ and $\overline{m_n} = m_n(1-\delta_1)$. One requires a value of about -0.009 for δ_1 (a 1.8% increase in the neutron mass

TABLE I. Values of the SKX Skyrme parameters obtained. They are compared with the results (SKXce) with the Coulomb exchange and without ^{48}Ni in the fit, and the results (SKXm) with $\alpha=1/3$. They also are compared with the previous SKP [55] and SkSC4 [56] interactions.

Parameter	SKXce	SKXm	SKX	SKP	SkSC4
α	0.5	1/3	0.5	1/6	1/3
x_w	0	0	0	1	1
x_c	1	0	0	1	1
χ	0.65	0.91	0.72		
t_0	−1438.0	−1803.1	−1445.3	−2931.7	−1789.4
t_1	244.3	273.8	246.9	320.6	283.5
t_2	−133.7	− 95.9	−131.8	−337.4	−283.5
t_3	12116.3	12755.1	12103.9	18709.0	12782.3
W_0	145.7	155.9	148.6	100.0	124.9
x_0	0.288	0.306	0.340	0.292	0.79
x_1	0.611	0.225	0.580	0.653	−0.5
x_2	0.145	0.698	0.127	−0.537	−0.5
x_3	−0.056	0.116	0.030	0.181	1.139
m^*/m	0.99	0.97	0.99	1.0	1.0
K	270	238	270	200	234
BE(^{176}Sn)	1158.0	1149.1	1149.0	1161.1	1156.3

relative to the proton mass). There is some discussion in the literature about the nuclear medium dependence of the isovector effective mass [30], but it is not clear how these models are related to the present result.

Another way that works is to drop the exchange correction to the Coulomb potential by setting x_c equal to zero in Eq. (3). If x_c is included as a fit parameter, then the minimum in the χ value is close to $x_c=0$. The results reported here are those obtained with $x_c=0$. Slightly better agreement for the $A=48$ binding energy difference can be obtained by allowing the strength of the Coulomb exchange to be varied or by allowing for an isovector effective mass. However, until one has a justification for doing one or the other, I prefer the simplicity and utility of just removing the exchange term.

It turns out that if the binding energy of ^{48}Ni is not included in the fit, then an equally good χ value is obtained with the usual $x_c=1$ but with a small change in the values of the other parameters (see SKXce in Table I). It is only when the binding energies of proton-rich nuclei are also considered that the introduction of the charge-asymmetric potential becomes important.

V. RESULTS FOR THE FIT

I consider the twelve parameters t_0, t_1, t_2, t_3, W_0, x_0, x_1, x_2, x_3, x_c, x_w, and α. As discussed above, $x_c=0$ was chosen in order to reproduce the displacement energy difference between ^{48}Ni and ^{48}Ca. The spin-orbit exchange parameter x_w is mainly determined by the spin-orbit gap in the single-particle states. When x_w is used in the fit, the minimum in the χ value is near $x_w=0$. The χ is about 20% larger with $x_w=1$. Thus I adopt the value $x_w=0$ which is close to the isoscalar form expected in the relativistic mean-field model [10]. I have not explored the possibility of using a density-dependent spin-orbit interaction [31], however, the fits to the single-particle energies I consider (see Sec. VI and Figs. 4–9) are very well reproduced by the present formulation. It is likely that this isoscalar form of the spin-orbit potential will lead to the reduced spin-orbit splitting in neutron matter which is suggested in Ref. [32], but I have not yet explicitly checked this.

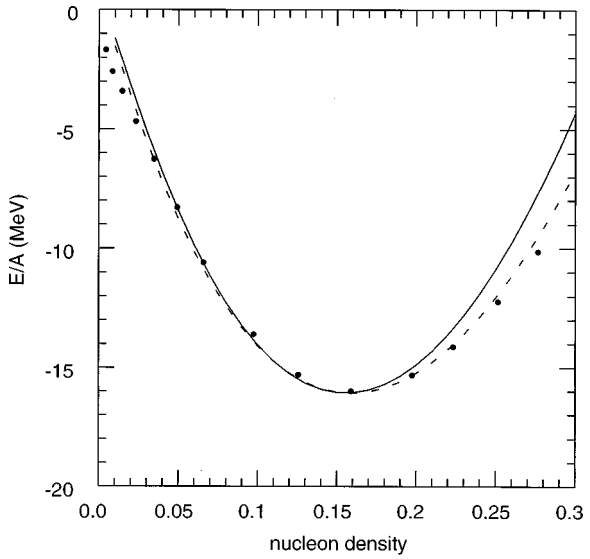

FIG. 1. E/A vs density (in units of nucleons/fm^2) for nuclear matter. The variational calculations for Friedman and Pandharipanda (filled circles) are compared with the present Skyrme interaction results with $\alpha=1/3$ (dashed line) and $\alpha=0.5$ (solid line).

With the remaining set of ten parameters, I find that six of them are well determined by the above set of data, namely, t_0, t_1, t_2, t_3, x_0, and W_0. I now discuss how the remaining parameters α, x_1, x_2, and x_3 are determined.

The least squares fit is not very sensitive to α with the χ vs α curve having a minimum of about $\chi=0.71$ in the range $\alpha=0.5$ and 0.8. At the upper range of α, the agreement between the experimental and theoretical SPE of ^{208}Pb becomes worse. There is a general tendency in all of these fits for some of the light nuclei to have a theoretical binding energy which is too large (for example at $\alpha=0.5$ the binding energy of ^{24}O is 1.8 MeV too large), and this trend is worse at the lower range of α. However, I put less emphasis on the deviations for light nuclei because the HF approximation should be better for heavy nuclei. Also there is a larger error in the harmonic-oscillator approximation to the center-of-mass correction for light nuclei.

The shape of the nuclear matter curve for E/A vs ρ (see Fig. 1) and the related incompressibility $K=9\rho^2 d^2E/d^2\rho|_{\rho=r_0}$ is sensitive to α. Over the range $\alpha=0.5$ to 0.8 the incompressibility varies from about 270 to 330 MeV. The value of K obtained from other experiments is at the lower range of these values, for example, $K=240$ to 270 MeV from a recent analysis of alpha-nucleus and nucleus-nucleus scattering data [33]. The three-nucleon part of the Friedman-Pandharipanda (FP) nuclear matter calculations [34] was fitted to give the $K=240$ MeV value inferred from the energies of the giant monopole resonances [35].

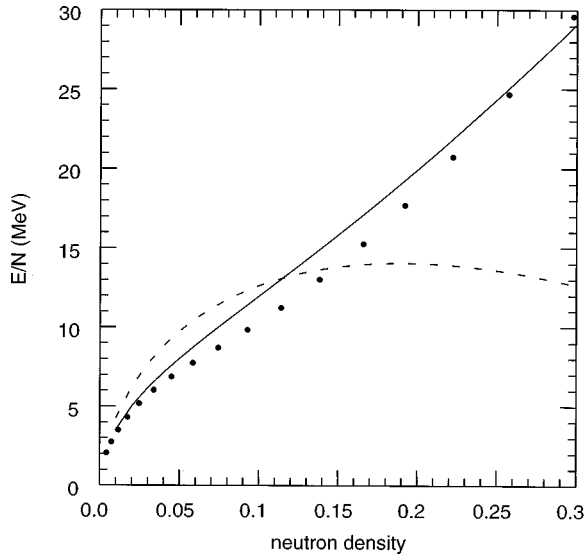

FIG. 2. E/N vs density (in units of neutrons/fm^3) for neutron matter. For the neutron matter, the variational calculations are compared with the present Skyrme interaction results with SKX ($x_3 = 0.03$) (line) and with another interaction which gives about the same fit to nuclear data but has $x_3 = 0.9$ (dashed line).

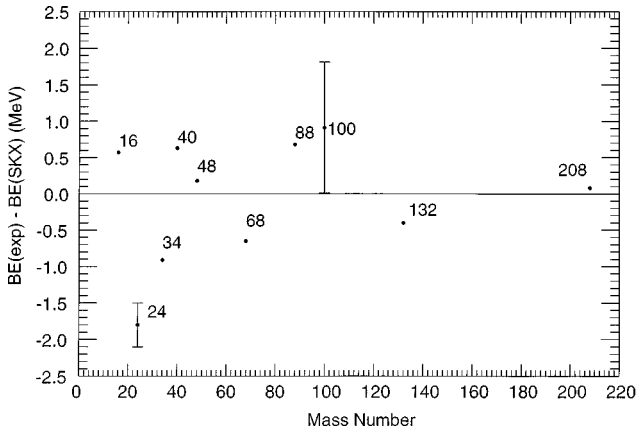

FIG. 3. Differences between the experimental and the theoretical binding energy for the nuclei considered in the fit. The experimental errors are small except for those of ^{24}O and ^{100}Sn. $A=48$ represents the result for ^{48}Ca. The result for ^{48}Ni is discussed in the text.

Thus, with a bias toward fitting the FP nuclear matter curve and having a smaller incompressibility, I have chosen $\alpha=0.5$ which gives $K=270$ MeV. When this Skyrme interaction is used for an RPA calculation of the monopole resonance in ^{208}Pb, the energy is about 10% too high [36]. The nuclear matter result as shown in Fig. 1 is that the FP curve is reproduced extremely closely from $\rho = 0.04$ to 0.17 nucleons/fm^3. Below $\rho=0.04$ nucleons/fm^3 the FP curve is more bound, which may be due to a long-range attraction which is missing in the Skyrme expansion. Above $\rho=0.17$ nucleons/fm^3, the FP curve is again more attractive, but it should be remembered that FP includes some phenomenological three-body forces which are adjusted to reproduce the extrapolated nuclear matter properties.

For a fixed value of α, the parameters t_0, t_1, t_2, t_3, x_0, and W_0 are varied to obtain a minimum in the χ. An equally good fit to all data can be obtained for a wide range of x_1, x_2, and x_3 values, but the fitted parameters depend upon their value. Unfortunately the location of the neutron drip line is rather sensitive to these undetermined parameters, in particular to x_3.

It turns out that the E/N vs ρ curve for *neutron* matter is extremely sensitive to x_3, as has been pointed out in Refs. [37] and [38]. Thus, if I include some points along the FP neutron matter curve in the fit with a 10% error, the value of x_3 becomes rather well determined and one can obtain a neutron matter curve which is very close to FP as shown in Fig. 2. If one tries to constrain the fit to neutron matter more tightly by putting, for example, a 1% error on the FP points, the χ value from the fit to the nuclear properties increases by about a factor of 2. So there is an indication in the present fit that the FP neutron matter calculations are not quite right. Indeed, it appears that a three-nucleon interaction could increase the FP points by about 10 percent in the range of $\rho = 0.10$ to 0.15 neutrons/fm^3 [39]. The sensitivity of the neutron matter curve to x_1 and x_2 is not large, and the location of the neutron drip line is also less sensitive to these. I include x_1 and x_2 in the fit to the nuclear and neutron matter properties, but their errors are large and an equally good fit could be obtained by setting them equal to zero. In the future one may be able to put further constraints on these x parameters from a consideration of the other giant resonances and the related empirical values of the Landau parameters [40].

With the above set of parameters ($\alpha=0.5$) a remarkably good fit with $\chi\approx0.73$ is obtained for the entire set of data considered; this interaction will be denoted by SKX. The values of the parameters for this interaction are given in Table I. Although one can easily obtain the uncorrelated parameter uncertainties from the fit, they are not very meaningful since the errors are dominated by the correlations between the parameters. For comparison I also give the results SKXce obtained with normal Coulomb exchange ($x_c=1$) and without ^{48}Ni in the fit. The nuclear matter effective mass which comes out of SKX and SKXce fits is $m^*/m=0.99$.

The results for the fit obtained with the even lower value of $\alpha=1/3$ gives a larger χ value of 0.91. The results labeled SKXm (for monopole fit) are given in Table I. The larger χ value comes mainly from the SPE in heavy nuclei being a little too spread out compared to experiment and this is related to a slightly smaller effective mass of $m^*/m=0.97$ which comes out of the fit. However, for the monopole giant resonance, the SKXm parameter set with a lower value of α which gives $K=238$ MeV might be preferred. For nuclear matter the main difference with the $\alpha=1/3$ result is that it is closer to the FP points at higher density (see Fig. 1). With $\alpha=1/3$ the calculated binding energy of ^{24}O comes out 2.3 MeV too large and the rms charge radius for ^{16}O comes out 0.02 fm too large compared to experiment.

VI. RESULTS FOR THE BINDING ENERGIES AND SINGLE-PARTICLE ENERGIES

The deviation between the experimental and theoretical binding energies for the nuclei chosen for the fit are shown in Fig. 3. The $A=48$ point shown in Fig. 3 is for ^{48}Ca. The overall rms is 0.82 MeV. The calculated value for the difference BE(^{48}Ca) $-$ BE(^{48}Ni) is $=$ 66.30 MeV compared to

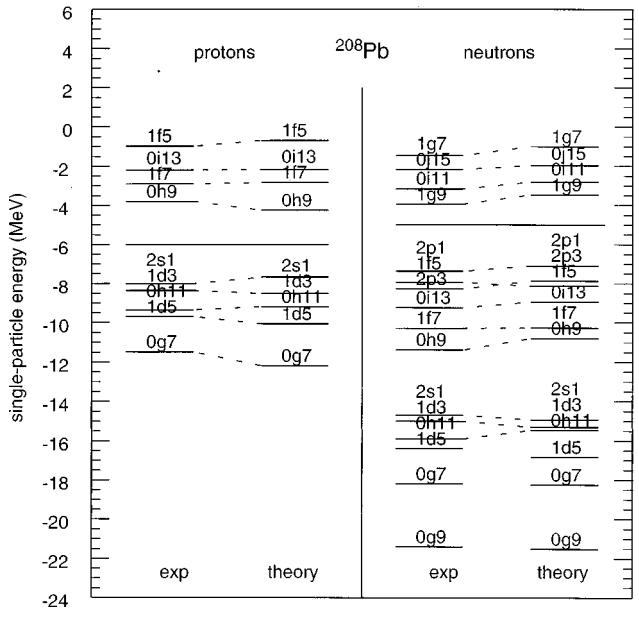

FIG. 4. Comparison of the experimental and theoretical (SKX) single-particle levels in ^{208}Pb. The levels connected by a dashed line were included in the fit. The labels are $(n,l,2j)$. The long solid lines indicate the division between particle and hole states.

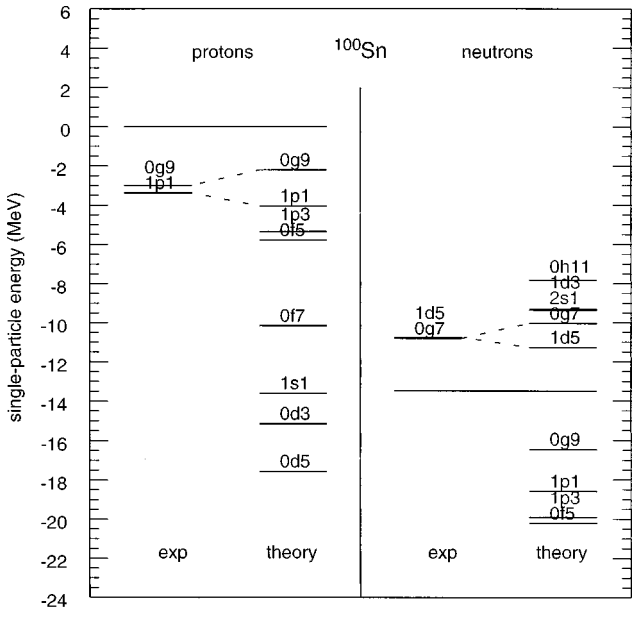

FIG. 6. Comparison of the experimental and theoretical (SKX) single-particle levels in ^{100}Sn. See caption to Fig. 4.

the experimental value of 67.06 MeV. As discussed above, this is the result obtained by turning off the exchange part of the Coulomb potential. If the exchange term is included, the theoretical binding energy difference is 62.7 MeV. Even though less weight was put on the ^{16}O and ^{40}Ca binding energies, the agreement with experiment for these two is typical of that for the other light nuclei.

The comparison between experiment and theory for the ^{208}Pb, ^{132}Sn, ^{100}Sn, ^{88}Sr, ^{48}Ca, ^{40}Ca, and ^{16}O single-particle energies are shown in Figs. 4–9. The rms deviation for the single-particle energies decreases with increasing mass with results for the rms of 1.7 MeV for ^{16}O, ^{34}Si, and ^{40}Ca, 0.84 MeV for ^{48}Ca, ^{88}Sr, and ^{100}Sn, 0.49 MeV for ^{132}Sn, and 0.35 MeV for ^{208}Pb. The large deviation for the lightest nuclei cannot be removed with any reasonable adjustment of the Skyrme parameters. These rms deviations were used to determine the theoretical errors discussed above for the data set. If I had used, for example, the same error of 0.5 MeV for all single-particle energies, the resulting rms deviations remain about the same as the above as a function of mass and the χ value goes up by about a factor of 2.

There are five loosely bound particle states not shown in Fig. 4 for ^{208}Pb, namely, those for the $2p_{3/2}$ and $2p_{1/2}$ proton states and the $2d_{5/2}$, $2d_{3/2}$, and $3s_{1/2}$ neutron states. These five levels are about 1 MeV lower in energy experimentally

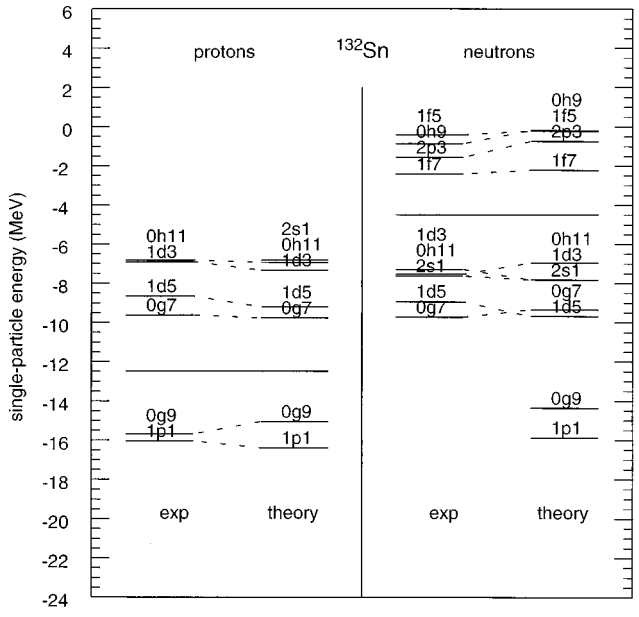

FIG. 5. Comparison of the experimental and theoretical (SKX) single-particle levels in ^{132}Sn. See caption to Fig. 4.

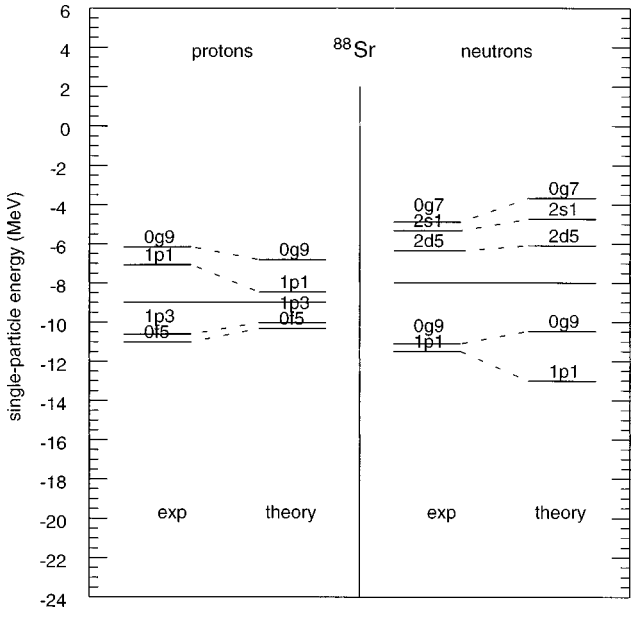

FIG. 7. Comparison of the experimental and theoretical (SKX) single-particle levels in ^{88}Sr. See caption to Fig. 4.

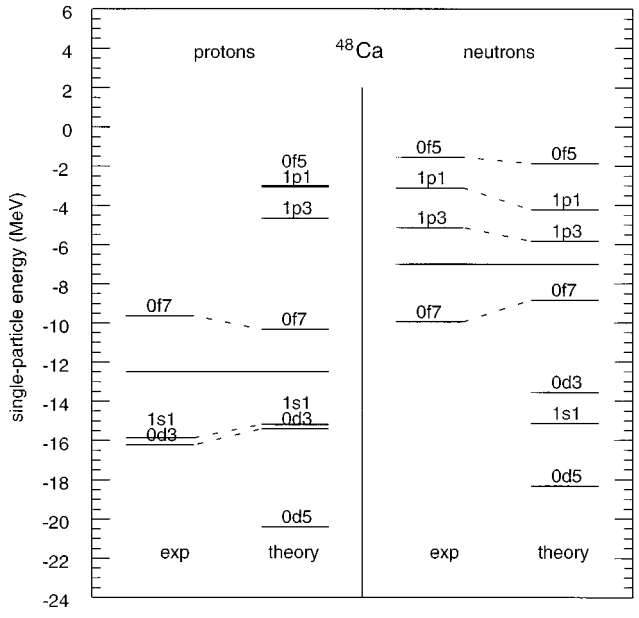

FIG. 8. Comparison of the experimental and theoretical (SKX) single-particle levels in ^{48}Ca. See caption to Fig. 4.

as compared to the theory. For example, the experimental $3s_{1/2}$ SPE is -1.91 MeV as compared to the SKX value of -0.65 MeV. This problem remains essentially the same for all of the varieties of Skyrme parameters I investigated in the course of this study. All of these low-l states are loosely bound and have a large rms radius. Thus, I speculate that the Skyrme potential is a little too weak at large radii due to the p-wave cutoff in the expansion, and that this is the reason why these states are theoretically underbound. This is consistent with the observation that the SKX nuclear matter binding energy at low density is too small compared to the FP variational calculations (see Fig. 1). However, the problem may also be associated with the spreading of the single-particle strength for these nl_j values to states at higher energy which have not yet been observed experimentally. These five states in ^{208}Pb were included in the fit with a theoretical error of 1.0 MeV and were not included in the 0.35 MeV rms deviation quoted above. There is a similar situation in ^{132}Sn with the loosely-bound $2p_{3/2}$ and $1f_{5/2}$ neutron states (see Fig. 5). These were also given a 1 MeV theoretical error in the fit.

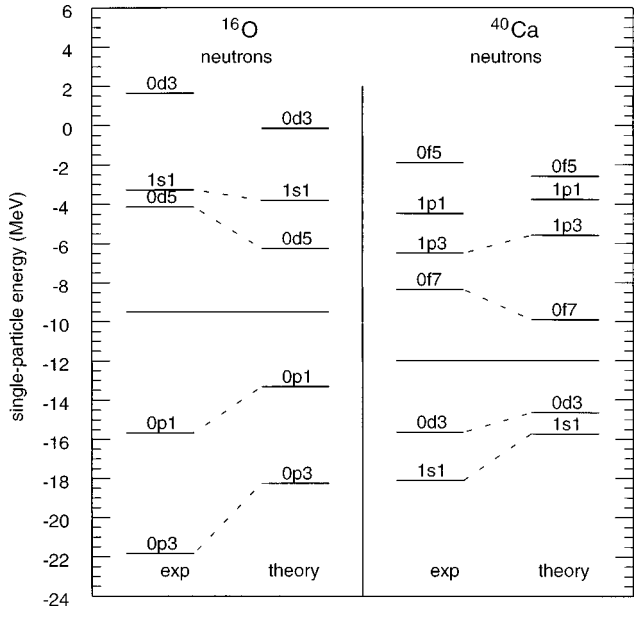

FIG. 9. Comparison of the experimental and theoretical (SKX) single-particle levels in ^{16}O and ^{40}Ca. See caption to Fig. 4.

It is interesting to note that energies for the three deepest neutron hole states ($0g_{9/2}$, $0g_{7/2}$, and $1d_{5/2}$) observed by Gales *et al.* [22] which were not included in the fit are well reproduced by the calculation. This good agreement for the deep-hole states tends to reinforce the need for the SKX effective mass m^*/m value of near unity. The deep hole states observed in light nuclei [41] (which are not in the fit) require a smaller effective mass of about 0.8 and are thus not reproduced by the SKX interaction. It is impossible with the Skyrme interaction to get agreement for both the ^{208}Pb SPE and those for the deep-hole states in light nuclei. Since the present work is designed to provide a starting point for shell-model configuration mixing of orbitals near the Fermi surface, one needs an effective mass near unity.

The quality of the comparison between the theoretical and experimental SPE for ^{132}Sn is comparable to that of ^{208}Pb. As mentioned above, the agreement between the experimental and calculated SPE becomes somewhat worse for ^{100}Sn, ^{88}Sr, and ^{48}Ca, but there are systematic differences. For example, the splitting between the $1p_{1/2}$ and $0g_{9/2}$ orbitals is always larger in the calculations compared to experiment. The $Z=38$ proton shell gap for ^{88}Sr is not very large and this will lead to an enhanced mixing across the gap which will be reflected in less pure single-particle states. The BCS calculations for the ^{88}Sr proton states given in Ref. [8] do not appear to improve the agreement.

The classic signature of mixing across the gap is the larger experimental ''quasiparticle'' gap compared to the calculated single-particle shell gap. This can clearly be seen in ^{48}Ca, ^{40}Ca, and ^{16}O. A nice example of how this effect can be accounted for by configuration mixing was shown by Gloeckner and Lawson [24] in the example of ^{12}C, where the experimental quasiparticle gap is nearly twice as large as the single-particle gap. This is due to the ground state correlations induced by excitations from the $0p_{3/2}$ to the $0p_{1/2}$ orbital. If one has a pure $(0p_{3/2})^8$ configuration, then the $0p_{3/2}$ ''hole'' spectroscopic factor in ^{13}C and the $0p_{1/2}$ ''particle'' spectroscopic factor in ^{11}C are both zero. When the simple configuration is broken by considering the full $(0p_{3/2}, 0p_{1/2})^8$ configuration space, these are no longer zero. The bare SPE can be recovered from experimental data by making an energy-weighted sum over the total strength of both orbitals in both the ''particle'' ($A=13$) and ''hole'' ($A=11$) nuclei. The deviation between effective and bare SPE is related to the fact that the effective energy only takes into account the dominant piece of the spectroscopic strength.

The largest deviations between theory and experiment are for the SPE of ^{16}O and ^{40}Ca. I have found that the agreement cannot be significantly improved with any reasonable set of Skyrme parameters even if one restricts the fit to light nuclei or to $N=Z$ nuclei. It is known that core-excited admixtures are important for ^{16}O and ^{40}Ca from the data from nucleon pickup reactions [11,42], from large-basis shell-model calcu-

lations which allow for core breaking [43,44].

As an example, I will analyze the effect of core-excitations on the SPE of the $0f_{7/2}$ orbital. The experimental value used in the fit and shown in Fig. 9 is just the binding energy difference between ^{41}Ca and ^{40}Ca. However, one finds from the ^{40}Ca$(d,t)^{39}$K reaction experiment [42] that the $0f_{7/2}$ ''particle'' orbital has about a 0.07 occupation probability in ^{40}Ca leading to the first $7/2^-$ state in ^{39}K. Taking the centroid of this $0f_{7/2}$ hole strength together with the dominant $0f_{7/2}$ particle strength in ^{41}Ca gives an SPE which is about 0.7 MeV lower than the ''bare'' value used in the fit—in the right direction to explain the deviation shown in Fig. 9.

The mixing across the gap appears to be more important for $N=Z$ nuclei compared to those with a neutron excess. This is probably related to the importance of α cluster excitations across the gap, as is evident in the well-known low-lying $4p$-$4h$ excitations in ^{16}O and ^{40}Ca [43,44]. The α cluster excitations are large because of the enhanced proton-neutron interaction between two protons and two neutrons in the same Nilsson orbitals. When there is a significant neutron excess as in ^{48}Ca, the lowest states for the two-proton excitation are different from those for the two-neutron excitation and the interaction is not as large. As mentioned above, there must be a certain amount of $2p$-$2h$, $4p$-$4h$, etc., excitations present in the ground states of all nuclei, and the average effect of these are renormalized into the effective Skyrme interaction. The difference for nuclei with $N=Z$ is that the $4p$-$4h$ (α cluster) excitations are larger than average. These effects are presumably also important for ^{100}Sn, but they are not so obvious from the comparison with the extrapolated single-particle energies [20] in Fig. 6. It will be important to have some direct experimental data for the masses and single-particle levels around ^{100}Sn.

Given that the SPE for ^{16}O and ^{40}Ca are not well described by SKX it is somewhat surprising that the binding energies for these two nuclei are only off by 0.6 MeV (see Fig. 3). However, this agreement may be accidental. If one were to take ^{24}O and ^{34}Si as better examples of closed-shell configurations, then the negative deviation for these (see Fig. 3) indicates that the SKX interaction systematically overbinds light nuclei. (The $0\hbar\omega$ correlation corrections for these nuclei discussed in Sec. III would make the calculated binding energies greater and the difference with experiment even larger.) With this interpretation one would take, for example, $[\mathrm{BE(exp,}^{16}\mathrm{O)}-\mathrm{BE(SKX,}^{16}\mathrm{O)}]-[\mathrm{BE(exp,}^{24}\mathrm{O)}-\mathrm{BE(SKX,}^{24}\mathrm{O)}]=2.4$ MeV as a measure of the extra binding (larger correlation energy) in ^{16}O.

VII. CHARGE RADII AND CHARGE DENSITIES

The difference between the experimental [19,45] and theoretical rms charge radii for even-even nuclei are shown in Fig. 10. The numerical results for the five nuclei in the fit are ^{16}O (rms=2.747 fm), ^{40}Ca (rms=3.472 fm), ^{48}Ca (rms =3.485 fm), ^{88}Sr (rms=4.213 fm), and ^{208}Pb (rms=5.498 fm). Even though less weight was put on the ^{16}O and ^{40}Ca radii, the agreement with experiment for these two is as good as for the others. In addition to these five nuclei included in the fit, I also include the comparison for all even-even nuclei given in the experimental compilations [19,45]. (For the comparison of the rms radii between the closed shells I have used the BCS+HF method [46] with a constant pairing strength $G=2.15/\sqrt{A}$ MeV in order to smooth out the occupation numbers.) The deviations for the five nuclei included in the fit are among those points near the bottom of Fig. 10 whose deviation between experiment and theory is on the order of 0.01 fm. The deviations for those nuclei away from these ''spherical'' nuclei is always positive and reflects the increase in the rms charge radius due to deformation, both static and dynamic. In both cases the increase of the rms radius $\sqrt{\langle r^2\rangle}$ can be related to the $B(E2,0^+\rightarrow 2^+)$ to the low-lying 2^+ states [47,48]:

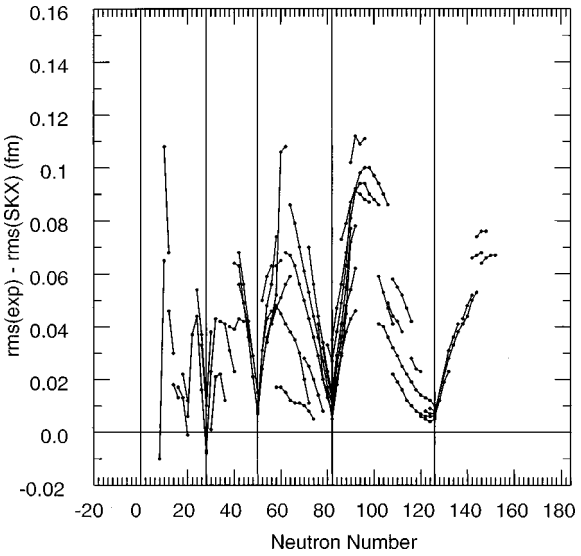

FIG. 10. The experimental rms charge radii [19,45] minus the calculated value for even-even nuclei. The comparison starts with ^{16}O and ends with ^{248}Cm. The data are plotted vs neutron number with those for a given Z value connected by a line. The vertical lines are for the magic numbers 28, 50, 82, and 126.

$$\langle r^2\rangle=\langle r^2\rangle_0\left(1+\frac{5\beta^2}{4\pi}\right) \tag{6}$$

and

$$B(E2)=\left[\frac{5Z\beta\langle r^2\rangle_0}{4\pi}\right]^2, \tag{7}$$

where $\sqrt{\langle r^2\rangle_0}$ is the rms radius of the equivalent spherical nucleus as obtained, for example, from the present spherical SKX calculation.

The largest deviations are those for the most statically deformed nuclei. For example, for ^{160}Gd with $B(E2)=52500\ e^2$ fm^4 [49], $Z=64$ and $\sqrt{\langle r^2\rangle_0}=5.066$ fm, I obtain $\beta=0.35$ from Eq. (7) and $\sqrt{\langle r^2\rangle}-\sqrt{\langle r^2\rangle_0}=0.12$ fm from Eq. (6), in excellent agreement with the largest difference at $N=96$ between the magic numbers 82 and 126 shown in Fig. 10. Further comparisons between the changes in radii and $B(E2)$ values are shown and discussed in Ref. [48].

The semimagic nuclei such as Sn (the lowest line of points between $N=50$ and $N=82$ in Fig. 10) and Pb (the lowest line of points between $N=100$ and $N=126$ in Fig. 10) show smaller increases away from the magic numbers

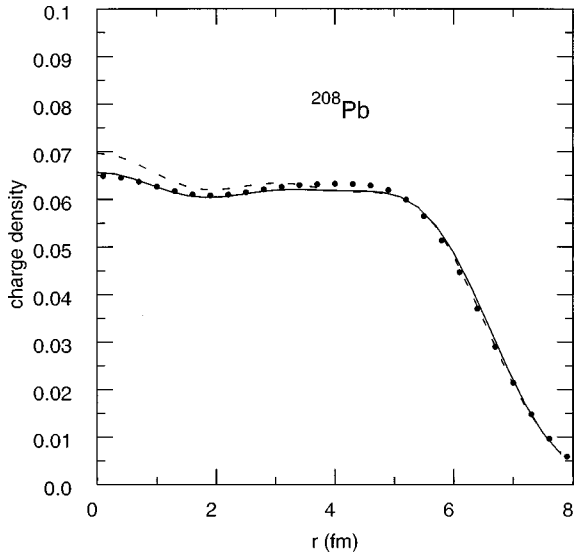

FIG. 11. The charge distribution for ^{208}Pb. The experiment (points) is compared with the calculated SKX distribution (solid line) and with a those from a typical Woods-Saxon distribution (dashed line). The experimental data is from the Fourier-Bessel decomposition given in Table IX of Ref. [19].

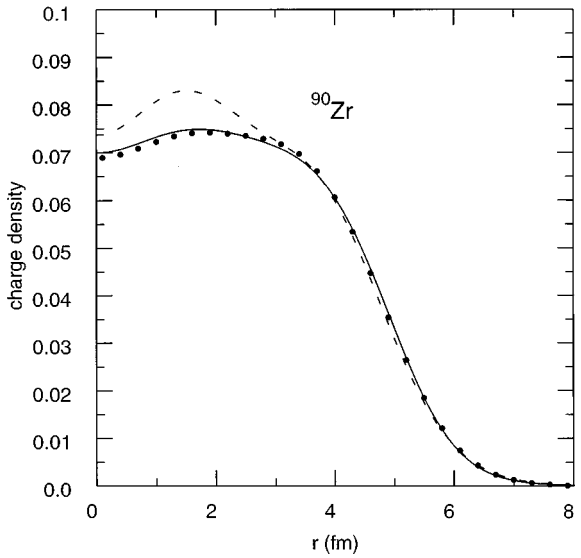

FIG. 12. The charge distribution for ^{90}Zr. See caption to Fig. 11.

which may also be related to the $E2$ strength to the lowest 2^+ states. The $E2$ strength for these valence neutron nuclei comes from the polarization of the core-protons by the valence neutrons [50]. For example, for ^{116}Sn, one finds $\beta = 0.11$ [49] and $\sqrt{\langle r^2\rangle} - \sqrt{\langle r^2\rangle_0} = 0.011$ fm, which is consistent with the small positive deviation observed in the middle of the Sn isotopes. The continued increase in the difference down to $N=56$ for the Sn isotopes indicates that the β value must continue to increase as one approaches ^{102}Sn, but these are not yet measured. A similar trend of increasing $B(E2)$ as one approaches ^{42}Ca is well known in the Ca isotopes which is related to the increased importance of core-excited admixtures as one approaches $N=Z+2$ [11].

Also the significant increase in the rms radius for the lightest Pb isotopes as well as for those just above ^{208}Pb indicates that these β are also large, but there is little experimental data on the $B(E2)$ values. There has been some discussion in the literature [10] about the influence of the Skyrme and relativistic potential parameters on the ''kink'' in the rms charge radii difference around ^{208}Pb. The systematics of the deviations in Fig. 10 show that this kink is a universal feature of the difference between experiment and spherical calculations at all magic numbers. One must consider the vibrational and deformed quadrupole correlations in order to fully understand their origin.

The isotopic dependence of the rms radii is dominated by the quadrupole deformation because the strength and excitation energy of this mode changes rapidly as a function of proton and neutron number. There must also be some lesser influences from the higher multipoles ($E3$, $E4$), but the low-lying strength for these modes does not show such strong shell effects. The vibrational correlations which are present even for the spherical nuclei [47], are to some extent renormalized into the effective Skyrme interaction.

The calculated and experimental [19] charge densities for ^{208}Pb, ^{90}Zr, and ^{48}Ca are shown in Figs. 11, 12, and 13, respectively. (The comparison is made for ^{90}Zr rather than ^{88}Sr because the Fourier-Bessel decomposition is given for the former in Ref. [19] and not for the latter.) The agreement is excellent for all three cases. One notices that the variety in the detailed structure of the interior oscillations is well reproduced by the calculations. For comparison I show some typical results based upon the Woods-Saxon potential [51,52] (dashed lines). The main difference between the HF and Woods-Saxon formulations is that the Hartree-Fock potential has self-consistent interior oscillations (rather than the flat Woods-Saxon form) which result in charge-density distributions which are in better agreement with experiment [51].

Some of the Skyrme interactions obtained by Friedrich and Reinhard [9] included the surface thickness of the charge distribution in their determination which led to a small value of the power of the density dependence of $\alpha = 0.25 - 0.35$. Although I have not included the surface thickness in the fit, one notices in Figs. 11–13 that the surface part of the charge

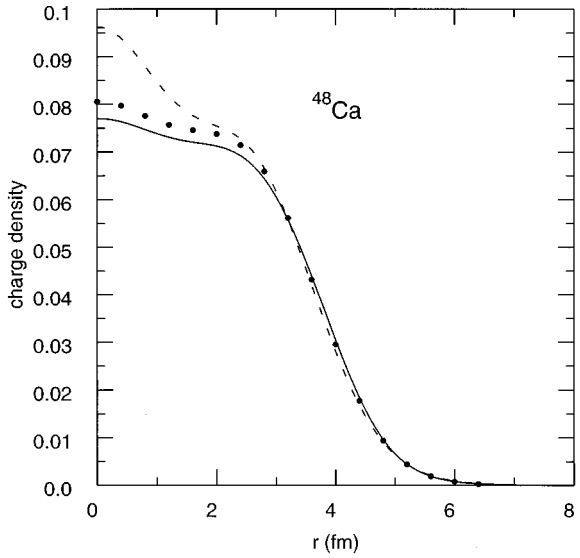

FIG. 13. The charge distribution for ^{48}Ca. See caption to Fig. 11.

distribution is well described by the calculations. As one goes away from these spherical nuclei, the quadrupole deformations which are responsible for the increase in the rms charge radii discussed above manifest themselves in the ground state density by an increase in the surface thickness. As discussed in Ref. [51], the small disagreement in the detail of the ^{208}Pb charge distribution may be due to the p-wave truncation of the nucleon-nucleon interaction which is inherent in the Skyrme ansatz or to nonclosed shell (higher-order) contributions to the charge density which cannot be fully taken into account by the simple density-dependent interaction.

VIII. CONCLUSIONS

The entire set of data considered here is remarkably well reproduced by the fitted Skyrme interaction SKX. Given the previous successes obtained with the Skyrme interaction this is not too surprising. What is important is that one can make further improvements in the formulation based upon the added information from single-particle energies, mirror nuclei, and neutron matter. There is still some room for improvement. The spin-orbit splittings are very well reproduced but the l centroids are systematically shifted. This together with the fact that the loosely bound states in ^{208}Pb are more bound experimentally than theoretically point to the fact that the surface properties of the Skyrme potential are not quite right. Perhaps the addition of a small d-wave term in the interaction would help.

As discussed in Sec. VI, an effective mass m^*/m of near unity is required to reproduce the single-particle energies near the Fermi surface. It is well known that the bare G matrix gives $m^*/m=0.7$ and that the enhancement towards unity is related to the coupling with the surface vibrations [53,54]. Many of the Skyrme interactions starting with the SII of Vautherin and Brink [2] give a small effective mass with the philosophy that further work must be done to take into account the surface vibrations. In contrast, the present Skyrme SKX has an effective mass near unity with the philosophy that all of the correlations at the closed shells are built into the effective Skyrme interaction and that the resulting mean field will provide an immediate starting point for shell-model configuration mixing of the orbitals near the Fermi surface. The freedom within the Skyrme interaction with regard to the effective mass was emphasized by Beiner *et al.* [8], and many Skyrme interactions, for example, SKP [55] and SkSC4 [56], have an effective mass of unity motivated by the desire to reproduce the level density at the Fermi surface. The full parameter set for the SKP and SkSC4 interactions are compared in Table I to the present results. The differences appear to be quite large, however, as emphasized in Sec. V, only six parameters are well determined by nuclear data and the consideration of nuclear and neutron matter properties are required in order to constrain α, x_1, x_2, and x_3. Even with the nuclear and neutron matter considerations, x_1 and x_2 are not determined and their values are strongly correlated with the t_1 and t_2 parameters.

The SKX interaction has unusual exchange properties the interpretation of which raises several unanswered questions. The small effective mass from the G matrix comes from the exchange term in the potential. Does the coupling to the surface vibrations provide an accidental cancellation to bring the effective mass back to unity, and to make it appear that the exchange term is missing? Also there is some preference in the fit for neglecting the exchange term of the Skyrme spin-orbit interaction. In addition, one way (of several) of accounting for the Nolen-Schiffer anomaly is to ignore the Coulomb exchange term. Are all of these things connected? Is this related to the fact that the actual nuclear ground state is rather complex and not just a single Slater determinant?

It is interesting to note that the result of not having all of these ''exchange'' terms produces a potential which is much like the Woods-Saxon formulation which has proven so useful in the early understanding of the nuclear mean field properties [57]. As discussed in Sec. VII, the main difference is that the Hartree-Fock potential has self-consistent interior oscillations (rather than the flat Woods-Saxon form) which produces charge-density distributions which are in much better agreement with experiment [51]. It is also interesting to note that the problems with the single-particle energies discussed for ^{16}O and ^{40}Ca appear in the same way in the early Woods-Saxon comparisons (compare Fig. 9 of this paper with Fig. 3–5 of Ref. [57]).

I have not included BCS correlations in the present fit because they are not important for the nuclei considered. Calculations for the semi-magic nuclei between the magic numbers require the introduction of BCS or HFB, and for the larger range of nuclei used for the comparison of Fig. 10, I used the HF+BCS method [46]. The spherical binding energies obtained in the HF+BCS approach are qualitatively similar to those shown in Fig. 14 of Ref. [8].

One can immediately make predictions for the most neutron-rich nuclei which could be doubly magic. The SKX binding energies for ^{60}Ca, ^{78}Ni, ^{176}Sn, and ^{266}Pb are 460.1, 642.3, 1149.0, and 1782.1 MeV, respectively. The SKX result for ^{78}Ni is in agreement with the Audi-Wapstra extrapolation of 641.4(1.1) MeV, perhaps confirming the doubly closed shell nature of this nucleus. The present results given above can be compared to the recent results obtained by Aboussir *et al.* [56] with the SkSC4 interaction of 454.3, 641.3, 1156.3, and 1798.9 MeV, respectively, for the set of nuclei given above. At the bottom of Table I I show the comparison of all of the interactions discussed in this paper for the binding energy of ^{176}Sn. These comparisons illustrate the difficulty and model dependence one has in making extrapolations for the properties of nuclei far from stability. Comparison of the SKX and SKXce binding energies shows that an understanding of the Nolen-Schiffer anomaly has an indirect influence on the properties of the most exotic neutron-rich nuclei, in addition to the direct influence on the properties of the proton-rich nuclei. Comparison of SKX and SKXm indicates that the binding energies of the most exotic nuclei are not very sensitive to α (and the related incompressibility) as long as the parameter set is constrained to the same set of data. The extrapolations are dependent upon the data set and the weights assigned to them. In order to improve the data set it would be most important to have an experimental value for the ^{78}Ni binding energy and a better measurement of the ^{100}Sn binding energy, both to an accuracy of about 100 keV.

The SKX interaction or an extension of it allows one to carry out HF calculations for the spherical nuclei at an accu-

racy which matches that of the configuration-mixed shell-model calculations for light nuclei [17] at the level of a few hundred keV for the binding energies and excitation energies. A complete microscopic model of nuclear structure might be based upon starting with the SKX mean field (or a similar suitable Skyrme interaction) and then adding the correlation energy due to the valence interactions, which includes the deformation driving proton-neutron interaction and the like-nucleon interactions (mainly pairing). It is interesting to try to derive the valence interactions from the Skyrme interactions [46,58], however, they may not be adequate since the valence spectra are sensitive to the higher multipole components of the interaction which are not determined from the closed shell data. At the most microscopic level the valence correlations can be treated by the large-basis shell-model methods for light nuclei [17] which are being extended to heavy nuclei with the Monte-Carlo methods [25,59,60]. Well-deformed heavy nuclei are probably best treated by the deformed HF method [56,61]. In addition, one might use the interacting-boson model for heavy nuclei [62], or at a more qualitative level, the N_p-N_n model [63] may be useful in understanding the dependence of the correlations between the closed shells in terms of the number of valence protons and neutrons.

ACKNOWLEDGMENTS

Support for this work was provided from U.S. National Science Foundation Grant No. PHY-9605207, the Alexander von Humboldt Stiftung, and the South African Foundation for Research and Development. I thank Werner Richter at Stellenbosch for his help and hospitality. I also thank Dr. J. Rikovska at Oxford University for helpful comments and for a program for the nuclear matter properties.

[1] T. H. R. Skyrme, Philos. Mag. **1**, 1043 (1956): Nucl. Phys. **9**, 615 (1959): **9**, 635 (1959).
[2] D. Vautherin and D. M. Brink, Phys. Rev. C **5**, 626 (1972).
[3] J. Treiner, M. Krivine, O. Bohigas, and J. Martorell, Nucl. Phys. **A371**, 253 (1981).
[4] S. Koehler, Nucl. Phys. **A258**, 301 (1976).
[5] J. Bartel, P. Quentin, M. Brack, C. Guet, and M. B. Hakannsson, Nucl. Phys. **A396**, 79 (1982).
[6] F. Tondeur, M. Brack, M. Farine, and J. M. Pearson, Nucl. Phys. **A420**, 297 (1984).
[7] M. Waroquier, K. Heyde, and G. Wenes, Nucl. Phys. **A404**, 269 (1984).
[8] M. Beiner, H. Flocard, Nguyen van Giai, and P. Quentin, Nucl. Phys. **A238**, 29 (1975).
[9] J. Friedrich and P.-G. Reinhard, Phys. Rev. C **33**, 335 (1986).
[10] M. M. Sharma, G. Lalazissis, J. Konig, and P. Ring, Phys. Rev. Lett. **74**, 3744 (1995).
[11] B. A. Brown, S. E. Massen, and P. E. Hodgson, Phys. Lett. **85B**, 167 (1979); J. Phys. G **5**, 1655 (1979).
[12] G. Audi and A. H. Wapstra, Nucl. Phys. **A595**, 409 (1995).
[13] B. A. Brown, Phys. Rev. C **43**, R1513 (1991); **44**, 924 (1991).
[14] B. J. Cole, Phys. Rev. C **54**, 1240 (1996).
[15] W. E. Ormand, Phys. Rev. C **53**, 214 (1996).
[16] M. Chartier *et al.*, Phys. Rev. Lett. **77**, 2400 (1996).
[17] B. A. Brown and B. H. Wildenthal, Annu. Rev. Nucl. Part. Sci. **38**, 29 (1988).
[18] W. A. Richter, M. G. Van der Merwe, R. E. Julies, and B. A. Brown, Nucl. Phys. **A523**, 325 (1991).
[19] G. Fricke, C. Bernhardt, K. Heilig, L. A. Schaller, L. Schellenberg, E. B. Shera, and C. W. de Jager, At. Data Nucl. Data Tables **60**, 177 (1995).
[20] B. A. Brown and K. Rykaczewski, Phys. Rev. C **50**, R2270 (1994).
[21] P. Hoff *et al.*, Phys. Rev. Lett. **77**, 1020 (1996).
[22] S. Gales, G. M. Crawley, D. Weber, and B. Zwieglinsky, Phys. Rev. C **18**, 2475 (1978).
[23] M. J. Martin, Nucl. Data Sheets **22**, 545 (1977).
[24] D. Gloeckner and L. Zamick, Phys. Rev. C **14**, 1662 (1976).
[25] T. Otsuka, M. Honma, and T. Mizusaki (unpublished).
[26] J. A. Nolen and J. P. Schiffer, Annu. Rev. Nucl. Sci. **19**, 471 (1969).
[27] E. H. Auerbach, S. Kahana, and J. Weneser, Phys. Rev. Lett. **23**, 1253 (1969).
[28] N. Auerbach, Phys. Rep. **98**, 273 (1983).
[29] B. A. Brown, MSU-NSCL annual report, 1996.
[30] T. Hatsuda, H. Hogassen, and M. Prakash, Phys. Rev. Lett. **22**, 2851 (1991); C. Adami and G. E. Brown, Z. Phys. A **340**, 93 (1991).
[31] J. M. Pearson and M. Farine, Phys. Rev. C **50**, 185 (1994).
[32] B. S. Pudliner, A. Smerzi, J. Carlson, V. R. Pandharipande, S. C. Pieper, and D. G. Ravenhall, Phys. Rev. Lett. **76**, 2416 (1996).
[33] D. T. Khao, G. R. Satchler, and W. von Oertzen, Phys. Rev. C **56**, 954 (1997).
[34] B. Friedman and V. R. Pandharipande Nucl. Phys. **A361**, 502 (1981).
[35] Y. W. Laui, P. Bogucki, J. D. Bronson, U. Garg, C. M. Roza, and D. H. Youngblood, Phys. Lett. **93B**, 31 (1980).
[36] G. Colo (private communication).
[37] C. J. Pethick, D. G. Ravenhall, and C. P. Lorenz, Nucl. Phys. **A584**, 675 (1995).
[38] C. J. Pethick and D. J. Ravenhall, Annu. Rev. Nucl. Part. Sci. **45**, 429 (1995).
[39] V. R. Pandharipande (private communication).
[40] G. A. Rinker and J. Speth, Nucl. Phys. **A306**, 360 (1978).
[41] F. Malaguti, A. Uguzzoni, E. Verondini, and P. E. Hodgson, Riv. Nuovo Cimento **5**, 1 (1982), and references therein.
[42] P. Doll, G. J. Wagner, K. T. Knopfle, and G. Mairle, Nucl. Phys. **A163**, 210 (1976).
[43] E. K. Warburton, B. A. Brown, and D. J. Millener, Phys. Lett. B **293**, 7 (1992).
[44] M. Sakakura, A. Arima, and T. Sebe, Phys. Lett. **61B**, 335 (1976).
[45] E. W. Otten, *Treatise on Heavy-Ion Science*, edited by D. A. Bromley (Plenum, New York, 1989), Vol. 8, p. 517.
[46] K. Heyde, *The Nuclear Shell Model* (Springer-Verlag, Berlin, 1990).
[47] H. Esbensen and G. F. Bertsch, Phys. Rev. C **28**, 355 (1983).

[48] B. A. Brown, C. R. Bronk, and P. E. Hodgson, J. Phys. G **10**, 1683 (1984).
[49] S. Raman, C. H. Malarkey, W. T. Milner, C. W. Nestor, and P. H. Stelson, At. Data Nucl. Data Tables **36**, 1 (1987).
[50] H. Sagawa, O. Scholten, B. A. Brown, and B. H. Wildenthal, Nucl. Phys. **A462**, 1 (1987).
[51] B. A. Brown, S. E. Massen, J. I. Escudero, P. E. Hodgson, and J. Vinas, J. Phys. G **9**, 423 (1983).
[52] J. Streets, B. A. Brown, and P. E. Hodgson, J. Phys. G **8**, 839 (1982).
[53] M. Jaminon and C. Mahaux, Phys. Rev. C **41**, 697 (1990).
[54] V. Bernard and Nguyen van Giai, Nucl. Phys. **A348**, 75 (1980).
[55] J. Dobaczewski, H. Flocard, and J. Treiner, Nucl. Phys. **A422**, 103 (1984): J. Dobaczewski, I. Hamamoto, W. Nazarewitcz, and J. A. Sheikh, Phys. Rev. Lett. **72**, 981 (1994).
[56] Y. Aboussir, J. M. Pearson, A. K. Dutta, and F. Tondear, At. Data Nucl. Data Tables **61**, 127 (1995); Nucl. Phys. **A549**, 155 (1992).
[57] A. Bohr and B. M. Mottelson, *Nuclear Structure* (Benjamin, New York, 1969), Vol. I.
[58] H. Sagawa, B. A. Brown, and O. Scholten, Phys. Lett. **159B**, 228 (1985).
[59] S. E. Koonin, D. J. Dean, and K. Langanke, Annu. Rev. Nucl. Part. Sci. **47**, 463 (1997).
[60] M. Honma, T. Mizusaki, and T. Otsuka, Phys. Rev. Lett. **77**, 3315 (1996).
[61] T. R. Werner, J. A. Sheikh, M. Misu, W. Nazarewicz, J. Rikovska, K. Heeger, A. S. Umar, and M. R. Strayer, Nucl. Phys. **A597**, 327 (1996).
[62] A. Arima and F. Iachello, Adv. Nucl. Phys. **13**, 139 (1984).
[63] D. S. Brenner, N. V. Zamfir, and R. F. Casten, Phys. Rev. C **50**, 490 (1994).